JOURNAL OF AIRCRAFT
Vol. 31, No. 6, November–December 1994

Moving Wall Effect in Relation to Other Dynamic Stall Flow Mechanisms

Lars E. Ericsson*
Mountain View, California 94040

An analysis is performed to determine the importance of the so-called moving wall effect relative to other unsteady flow mechanisms present in the dynamic stall process. Analysis of existing theoretical and experimental results indicates that the tangential moving wall effect on the initial boundary-layer development, close to the flow stagnation point, is not satisfactorily represented in current numerical methods. The analysis shows that this moving wall effect plays a dominant role in inducing self-excited oscillations, such as the wing rock of advanced aircraft, and also plays a significant role in so-called supermaneuvers of these aircraft.

Nomenclature

b = wing span
c = reference length, airfoil chord
f = frequency
K_1 = constant in Eq. (4)
K_2 = constant in Eq. (5)
L = wing lift, coefficient, $L/(\rho_\infty U_\infty^2/2)S$
l = rolling moment, coefficient, $l/(\rho_\infty U_\infty^2/2)Sb$
l' = sectional lift, coefficient, $l'/(\rho_\infty U_\infty^2/2)c$
M = freestream Mach number
m = sectional pitching moment, coefficient, $m/(\rho_\infty U_\infty^2/2)c$
n = sectional normal force, coefficient, $n/(\rho_\infty U_\infty^2/2)c$
p = roll rate
Re = Reynolds number, $U_\infty c/\nu_\infty$
r_N = airfoil nose radius
S = reference area, projected wing area
t = time
U = velocity
x = distance from the leading edge
z = translatory coordinate
α = angle of attack
α_0 = mean angle of attack
Δ = amplitude or increment
$\Delta\zeta$ = dimensionless amplitude, $\Delta z/c$
θ = perturbation in pitch
ν = kinematic viscosity
ξ = dimensionless x coordinate, x/c
ρ_N = dimensionless nose radius, r_N/c
ρ_∞ = air density
σ = inclination of roll axis
ϕ = roll angle
ω = angular frequency, $2\pi f$
$\bar{\omega}$ = dimensionless frequency, $\omega c/U_\infty$

Derivative Symbol
$\dot{\alpha}$ = $\partial\alpha/\partial t$; $C_{lp} = \partial C_l/\partial(pb/2U_\infty)$

Subscripts
CG = center of gravity or rotation
s,sep = separation
sh = shock
N = nose
W = wall
w = wake
1,2 = numbering subscripts
∞ = freestream conditions

Received Sept. 21, 1993; revision received March 15, 1994; accepted for publication March 28, 1994.

*Engineering Consultant, 1518 Fordham Way.

Introduction

IN view of the giant strides taken by computational fluid dynamics (CFD) in recent years, some may believe that the era forecast in Ref. 1 finally has arrived. The fact that there still will be some time before CFD can supplant the wind tunnel is not always made clear. Thus, in a recent paper on dynamic stall,[2] the following statement is made: "The important physical aspects of the flow development can be understood from experimental studies in this lower Reynolds number regime since many of the key features of the dynamics are common to a wider range of Reynolds number. Other work[3] also substantiates this conclusion." This statement contrasts sharply with the claim made in the conclusions of Ref. 4 that "Full scale unsteady aerodynamics cannot be simulated in dynamic tests at subscale Reynolds numbers, . . .". It can be surmised, therefore, that a careful definition is needed of "the key features of the dynamics" that are not critically dependent upon the Reynolds number. It will be shown that dynamic stall is critically dependent upon the Reynolds number in many cases of interest for high-performance aircraft.

Discussion

The time-lagged quasisteady or dynamically-equivalent steady (DES) aerodynamics, as defined in Refs. 4 and 5, are unsteady aerodynamics that can be derived by use of static experimental characteristics. Their relationship to static aerodynamic characteristics is defined by two parameters, viz., the phase lag of the static force vector and the change of its magnitude; the former is caused by the effect of convective time lag, and the latter is the result of dynamic improvement or degradation of the boundary-layer characteristics. For leading-edge stall, the stall type of most practical interest, the dynamic overshoot $\Delta\alpha_{sep}$ of the static stall angle α_s has the following two components[4,5]:

$$\Delta\alpha_{sep} = \Delta\alpha_w + \Delta\alpha_s \tag{1}$$

The component $\Delta\alpha_w$ is the delay of the circulation buildup due to von Kármán-Sears vortex-wake lag[5]

$$\Delta\alpha_w = 1.5\dot{\alpha}c/U_\infty \tag{2}$$

It delays the static characteristics, such as the lift, to occur at $\alpha + \Delta\alpha_w$. Contrary to what is the case for $\Delta\alpha_w$, the overshoot

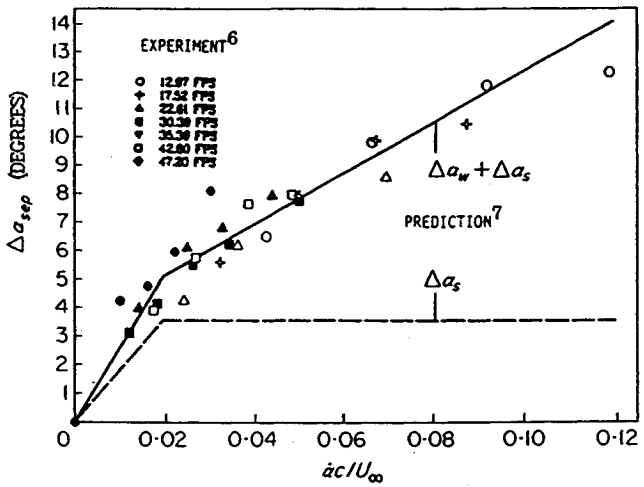

Fig. 1 Dynamic overshoot $\Delta\alpha_s$ of the static stall angle α_s at constant pitch-up rates.

$\Delta\alpha_s$ of the static stall angle results in an overshoot of the static lift maximum.

These DES effects delay the occurrence of flow separation. When separation finally occurs, important transient aerodynamic effects enter into the picture, all tied to the growth and "spillage" of the dynamic stall vortex from the leading-edge region.[5]

The DES effects on dynamic stall are well illustrated by the experimentally observed delay of flow separation at the quarterchord $\xi = 0.25$ on a NACA 0015 airfoil in a ramp-wise pitch-up motion[6,7] (Fig. 1). The significance of Fig. 1 is that until the boundary-layer improvement through accelerated-flow and moving-wall effects is saturated, at $\dot{\alpha}c/U_\infty > 0.02$ for rotation about the quarterchord ($\xi_{CG} = 0.25$), it more or less dictates when separation will occur, i.e., $\Delta\alpha_s >> \Delta\alpha_w$ in Eq. (1). However, at $\dot{\alpha}c/U_\infty > 0.02$, when the motion-induced improvement of the boundary-layer characteristics is saturated,[5] the delay $\Delta\alpha_w$ due to the time lag associated with the circulation buildup dominates over $\Delta\alpha_s$ in determining the overshoot $\Delta\alpha_{sep}$ over the static stall angle α_s.

The limiting value $\dot{\alpha}c/U_\infty = 0.02$, used in the analysis in Refs. 5 and 7 for the maximum value of $\Delta\alpha_s$, is based upon the experimental results in Ref. 8. A similar asymptotic behavior of the flow reversal is predicted by CFD[9] (Fig. 2). The earlier saturation of the moving wall effect in the experiment[8] is probably in large part caused by compressibility effects,[10] present in the experiment,[8] but not in the incompressible analysis of Ref. 9. In contrast, there is a very marked disagreement between the CFD data trends[3] in Fig. 3 and the experimental results[11] in Fig. 4. The CFD results[3] for $\dot{\alpha}c/U_\infty = 0.045$ in Fig. 3 predict the maximum lift to decrease as the rotation center is moved farther aft from the leading edge. This is in direct opposition to the experimental results[11] in Fig. 4 for $|\dot{\alpha}c/U_\infty| = \omega\Delta\theta \leq 0.06$, showing the experimental lift maximum to increase as the rotation axis is moved aft. The most likely reason for this opposition between predicted and experimental data trends is the pitch-rate-induced moving wall effect at the leading edge, i.e., the so-called LE-jet effect.[5]

As described in Ref. 5, the dynamic stall overshoot $\Delta\alpha_s$ has two components:

$$\Delta\alpha_s = \Delta\alpha_{s1} + \Delta\alpha_{s2} \tag{3}$$

The component $\Delta\alpha_{s1}$ is generated by the accelerated-flow effect on the ambient pressure-gradient time history. It is only determined by the rate of change of the angle of attack and can be written

$$\Delta\alpha_{s1} = K_1\dot{\alpha}c/U_\infty \tag{4}$$

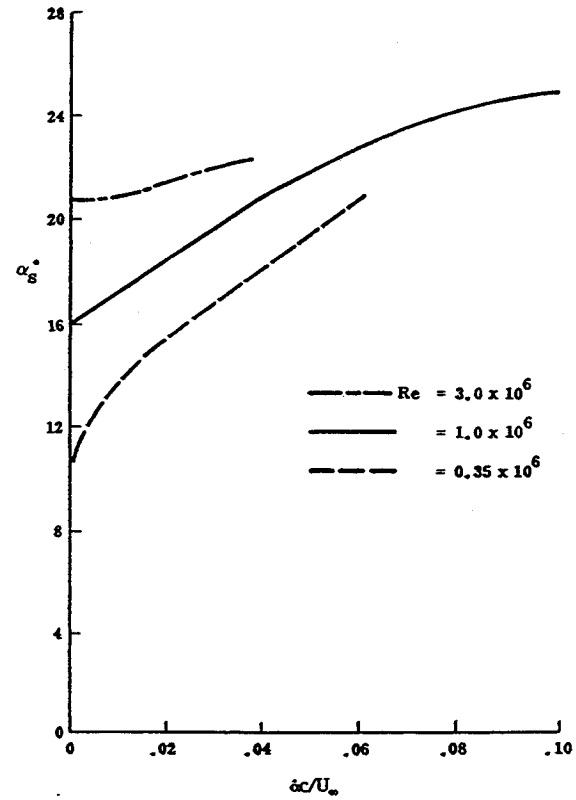

Fig. 2 Combined effect of Reynolds number and pitch-up rate on flow reversal.[9]

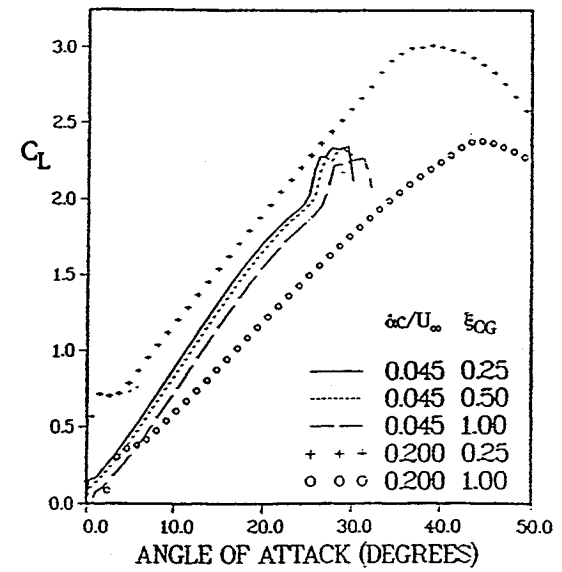

Fig. 3 Effect of pitch-up rate on wing lift.[3]

The other component, $\Delta\alpha_{s2}$, is generated by the LE-jet effect (Fig. 5). In a first approximation, $\Delta\alpha_{s2}$ is proportional to the LE-plunging velocity $\dot{z}_{LE}$, i.e.,

$$\Delta\alpha_{s2} = -K_2\dot{z}_{LE}/U_\infty \tag{5}$$

That is, for an airfoil pitching around ξ_{CG}

$$\Delta\alpha_s = \Delta\alpha_{s1} + \Delta\alpha_{s2} = K\dot{\alpha}c/U_\infty \tag{6a}$$

$$K = K_1 + K_2\xi_{CG} \tag{6b}$$

Based upon the relationship in Eq. (6), where K_1 and K_2 are positive constants, one expects the dynamic overshoot of

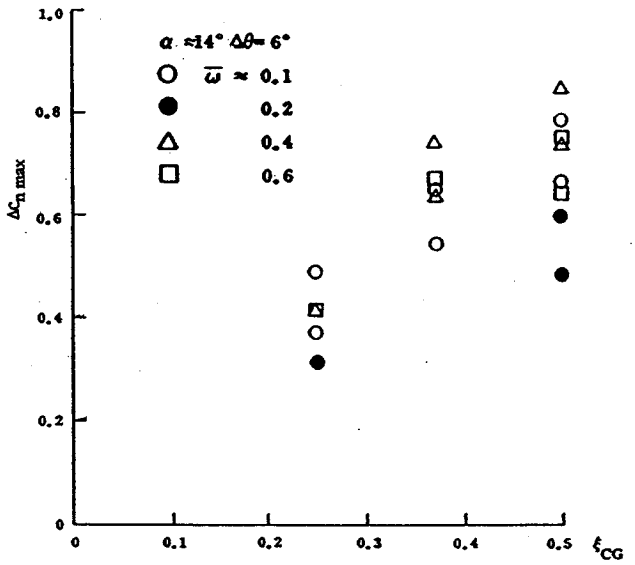

Fig. 4 Effect of oscillation center location on dynamic stall overshoot.[11]

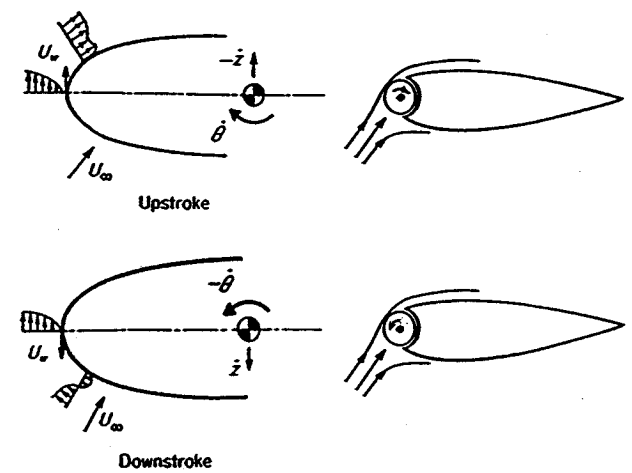

Fig. 5 The leading-edge-jet effect.[5]

static lift maximum to increase with increasing ξ_{CG}, in agreement with the experimental results[11] in Fig. 4.

Figure 5 illustrates the fact that for a pitching airfoil $\Delta\alpha_{s1}$ and $\Delta\alpha_{s2}$ are additive, as shown in Eq. (6), but are opposing each other for a plunging airfoil. That is, for plunging oscillations

$$\Delta\alpha_{s1} = K_1\dot{z}_{LE}/U_\infty \tag{7a}$$

$$\Delta\alpha_{s2} = -K_2\dot{z}_{LE}/U_\infty \tag{7b}$$

$$\Delta\alpha_s = \Delta\alpha_{s1} + \Delta\alpha_{s2} = (K_1 - K_2)\dot{z}_{LE}/U_\infty \tag{7c}$$

According to an analysis of experimental results,[12] $K_2 \approx 2K_1$. Thus, for a plunging airfoil the moving wall effect dominates, promoting dynamic stall, whereas stall is delayed for a pitching airfoil. As a consequence, plunging oscillations become undamped when stall occurs, as observed in tests by Liiva et al.[8] (Fig. 6). This can lead to the wing rock experienced by the X-29A aircraft.[13,14]

Reynolds Number Effects

The Reynolds number can be a very critical parameter. This is demonstrated by the experimental results for the NACA 0012 airfoil in plunging oscillations[8,15] (Fig. 7). It is described in Ref. 16 how the different damping-in-plunge measured at low[15] and high[8] Reynolds numbers (Fig. 7) can be explained by the moving wall effects on the boundary layer[5] (Fig. 5), which are very similar to those measured on a rotating circular

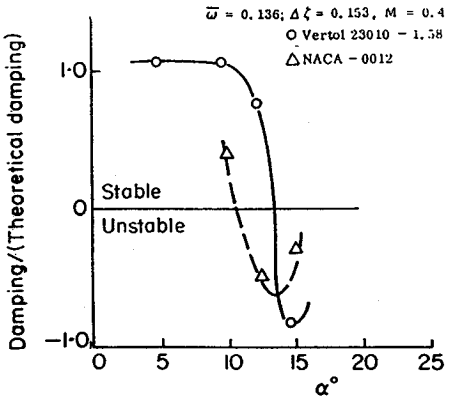

Fig. 6 Plunging-induced undamping.[8]

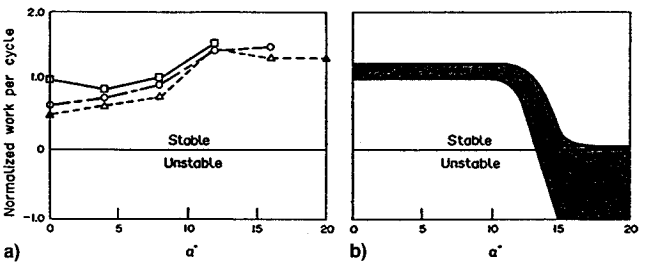

Fig. 7 Effect of Reynolds number on damping in plunge. $Re \approx$ a) 10^5 and b) 10^6 (Refs. 15 and 8, respectively).

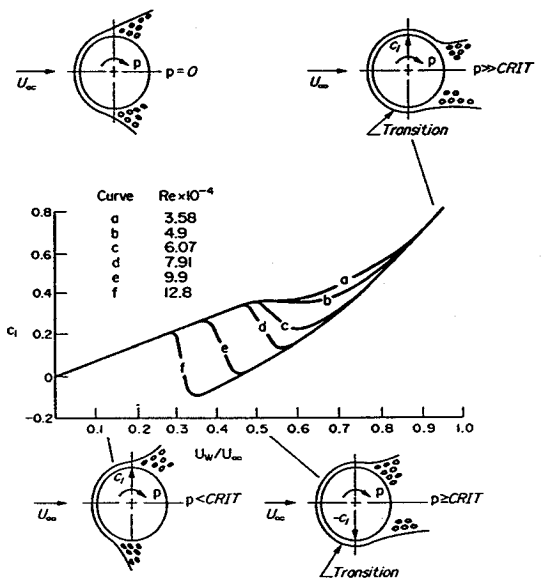

Fig. 8 Magnus lift characteristics for initially subcritical flow conditions.[17]

cylinder[17] (Fig. 8). The positive Magnus lift, at $U_w/U_\infty < 0.3$ in Fig. 8, is caused by the wall-jet-like downstream moving wall effect on the top side, which fills out the boundary-layer velocity profile, thereby delaying flow separation. A similar lift-contribution is obtained from the upstream moving wall effect on the bottom side, which promotes separation. At $U_w/U_\infty > 0.3$, so-called Magnus lift reversal occurs, when the critical combination of U_w/U_∞ and Reynolds number is exceeded, causing boundary-layer transition to occur upstream of flow separation, thereby changing the separation from the subcritical towards the supercritical type. This results in a more or less discontinuous loss of lift. The moving wall effect is of significant magnitude only in the region near the stagnation point, where the boundary layer is thin and, therefore, very sensitive to this wall-jet-like action.

A similar moving wall effect on boundary-layer transition occurs on airfoils. Figure 5 illustrates how the plunging and

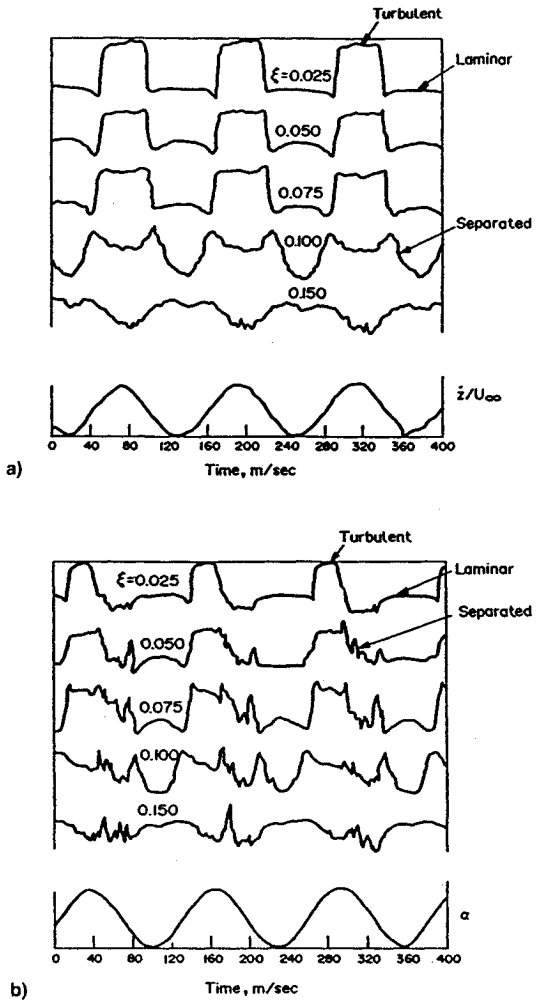

Fig. 9 Hot film response data for NACA 0012 airfoil[18]: a) plunging and b) pitching.

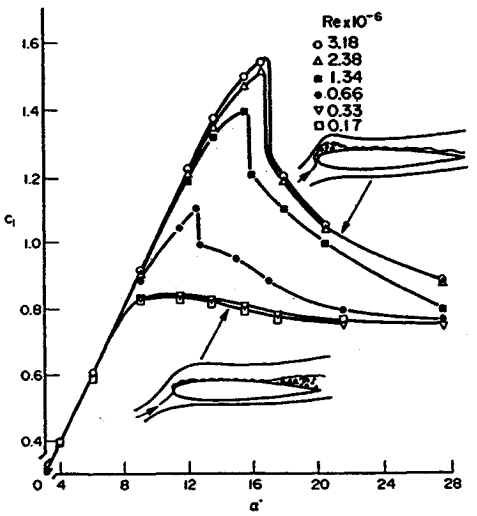

Fig. 10 Effect of Reynolds number on the lift characteristics of NACA 0012 airfoil.[20]

pitching airfoils will have opposite moving wall effects for increasing effective angle of attack, during the plunging downstroke $\dot{z}/U_\infty$ and the pitching upstroke θ, respectively. The accelerated flow effect, producing $\Delta\alpha_{s1}$, is determined by the motion-induced effect on the ambient pressure gradient at the edge of the boundary layer. It is the same for pitching and plunging oscillations as long as $\dot{z}_{LE}/U_\infty = \dot{\alpha}c/U_\infty$. Carta's hot film response data[18] (Fig. 9) show that as a result of the adverse (upstream) moving wall effect generated by $\dot{z}(t)$, transition is promoted, causing the plunging airfoil to have a longer run of attached turbulent flow prior to stall. As a result, the flow stays attached past 7.5% chord, whereas flow separation occurs forward of 5% chord on the pitching airfoil, which has a shorter turbulent run before stall due to the opposite, transition-delaying, moving wall effect. In addition to showing the opposite moving wall effects for pitching and plunging oscillations, Fig. 9 also demonstrates that the moving wall effect (K_2) completely dominates over the effect of the lessened pressure gradient adversity due to accelerated flow effects (K_1),[5] which is the same for pitching and plunging oscillations. This dominance is found in numerous flow situations both in two- and three-dimensional flow.[19]

These moving wall effects on transition explain the anomalous subscale test results obtained by Carta.[18] Like Rainey[15] (Fig. 7a) Carta failed to measure the negative damping in plunge that Liiva et al.[8] observed in their test, performed at an order of magnitude higher Reynolds number (Fig. 7b). Not only did Rainey and Carta fail to measure the negative damping expected at full-scale Reynolds numbers, the measured damping was actually 50–100% higher in the stall region than in the attached flow region. Instead of catching the discontinuous lift loss occurring at higher Reynolds numbers,[20] as in Liiva's test[8] (e.g., for $Re \geq 0.66 \times 10^6$ in Fig. 10), in Carta's and Rainey's tests the moving wall effect on the plunging downstroke has an effect similar to that of increasing the Reynolds number in Fig. 10, elevating the lift from, e.g., that for $Re = 0.33 \times 10^6$ to that for $Re = 0.66$ or 1.34×10^6. This causes the area enclosed by the plunging loop to be larger than for attached flow, resulting in the higher measured damping shown in Fig. 7a.

High-Alpha Aircraft Dynamics

Advanced aircraft are required to operate efficiently at high angles of attack. In the interim periods between performing "supermaneuvers," the aircraft often may be subject to wing rock. The aircraft designer needs to be able to predict the unsteady aerodynamics in both cases. The flow phenomena dominating the aerodynamics in the two cases are described in what follows.

Wing Rock

Figure 11 shows the wing-rock characteristics of the X-29 aircraft.[14] When the angle of attack exceeds 20 deg, the aircraft becomes dynamically unstable in roll (Fig. 11a). This is caused by the plunging-induced negative damping of the wing section discussed earlier (Fig. 6). Figure 11b shows the rapid increase of the wing-rock amplitude with increasing angle of attack. For the rolling wing, the effective angle of attack varies as follows:

$$\alpha(\phi) = \tan^{-1}(\tan\sigma\cos\phi) \tag{8}$$

Thus, when $\alpha(\phi) < \alpha_{reatt.}$, the plunging wing section starts generating positive damping. At the limit-cycle amplitude, the net damping is zero. Equation (7) shows how $\alpha(\phi)$ increases with increasing inclination σ of the roll axis, requiring higher and higher roll angle ϕ to reach the condition $\alpha(\phi) < \alpha_{reatt.}$, needed to limit the amplitude buildup of the wing rock. The fast increase of the wing-rock amplitude with increasing angle of attack for X-29A[14,21] (Fig. 11b) reflects this effect of increasing σ. It is obviously critical to be able to predict $\alpha_{reatt.}$ in order to determine the wing rock motion and its limit-cycle amplitude.

Supermaneuvers

It should be clear that self-excited oscillations, such as the X-29A wing rock, cannot be predicted unless the LE-jet effect is included in the computational method. However, according to the results in Fig. 1, the relative importance of this moving wall effect decreases with increasing pitch rate, becoming sat-

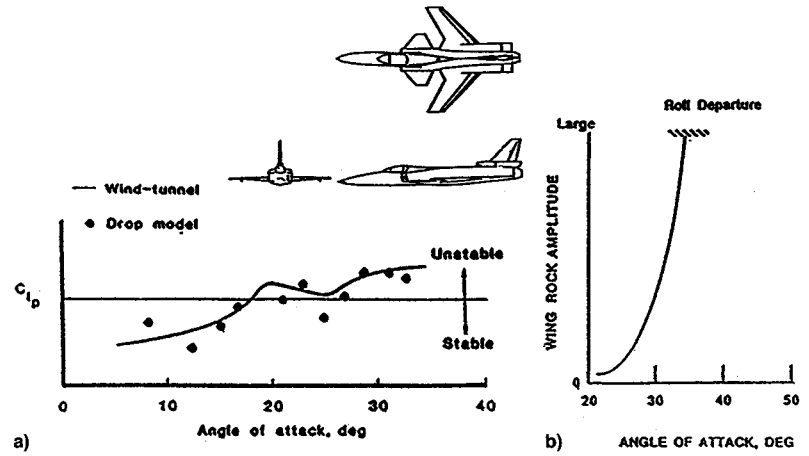

Fig. 11 Wing rock of the X-29 A aircraft[14]: a) roll damping and b) wing-rock amplitude.

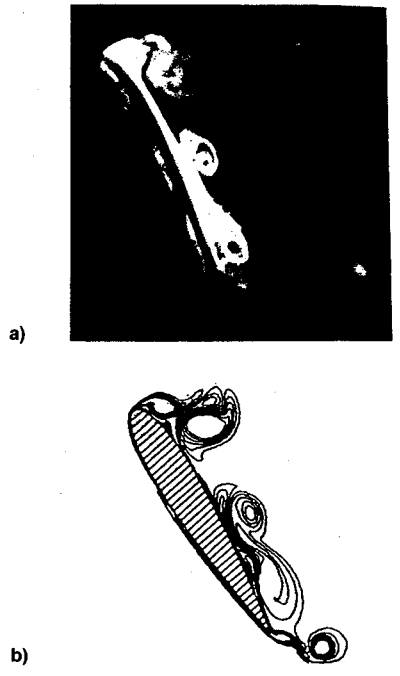

Fig. 12 Vorticity characteristics of NACA 0012 airfoil in pitch-up motion at $\dot{\alpha}c/U_\infty = 0.6$: a) experimental flow visualization[22] and b) numerical prediction.[3]

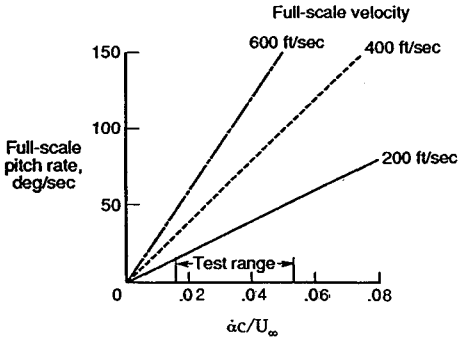

Fig. 13 Realistic range of pitch-up rates for current and future high-performance aircraft.[24]

urated at $\dot{\alpha}c/U_\infty > 0.02$. This explains the good agreement between CFD[3] and experiment[22] in Fig. 12 for the high pitch rate $\dot{\alpha}c/U_\infty = 0.6$. The question arises whether or not the high pitch rate ($\dot{\alpha}c/U_\infty = 0.6$) in Fig. 12 is representative of so-called supermaneuvers.[23] According to a recent review[24] (Fig. 13), it is not. Comparing Fig. 13 with Fig. 1, one finds

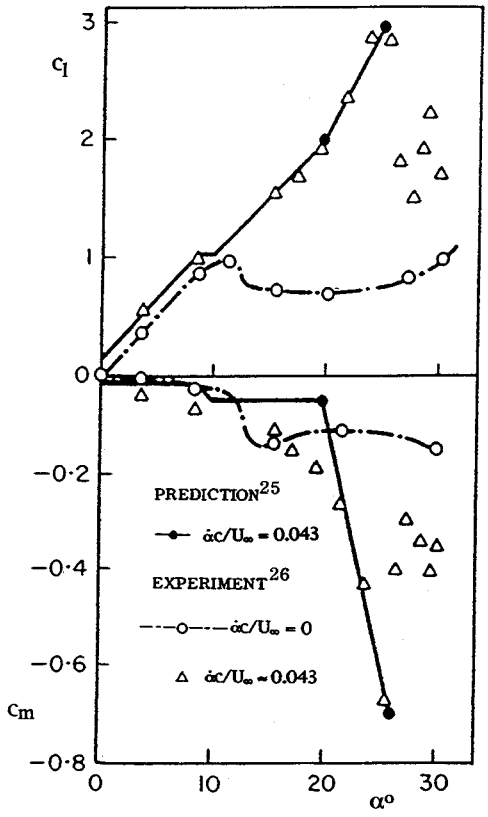

Fig. 14 Lift and pitching moment on NACA 0012 airfoil in pitch-up motion at $\dot{\alpha}c/U_\infty \approx 0.043$.

that for the test range in Fig. 13, which "allowed for a realistic representation of full-scale maneuvering conditions within the capabilities of current and future high performance airplanes,"[24] i.e., $0.015 < \dot{\alpha}c/U_\infty < 0.055$, the moving wall effect goes from dominant ($\Delta\alpha_s >> \Delta\alpha_w$) to being of roughly the same importance as the von Kármán-Sears wake lag ($\Delta\alpha_s \approx \Delta\alpha_w$). The results in Fig. 14 for a NACA 0012 airfoil in pitch-up motion at $\dot{\alpha}c/U_\infty \approx 0.043$ represent flight conditions close to the upper limit in Fig. 13. Figure 14 shows that the dynamic overshoot of static lift maximum depends to a roughly equal degree on dynamically-equivalent steady (10 deg $< \alpha <$ 20 deg) and transient ($\alpha >$ 20 deg) effects, according to both prediction[25] and experiment.[26]

The experimentally observed lift oscillation in Fig. 14 following the maximum lift one would be inclined to ascribe to the effects of vorticity time history, of the type illustrated by the CFD results[3] in Fig. 15 for $Re = 10^4$. However, before

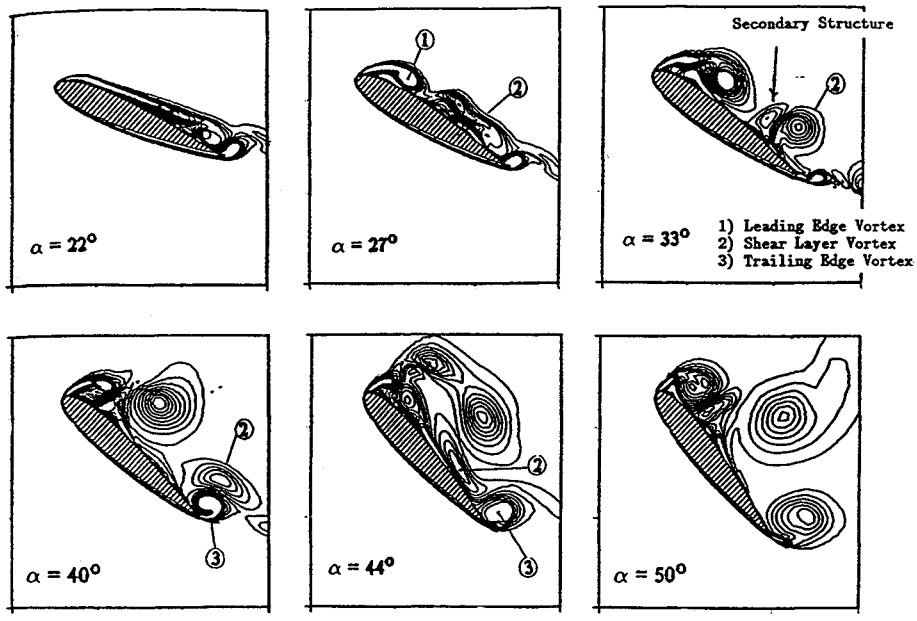

Fig. 15 Computed evolution of vorticity field on NACA 0015 airfoil in pitch-up motion at $\dot{\alpha}c/U_\infty = 0.20$, $Re = 10^4$ (Ref. 3).

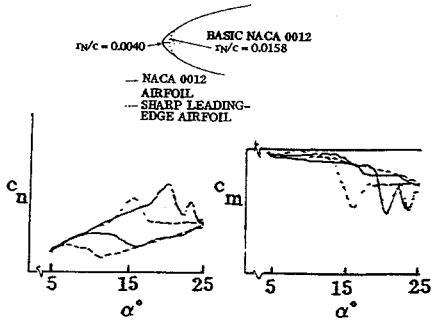

Fig. 16 Stall loops for basic and modified NACA 0012 airfoil.[27]

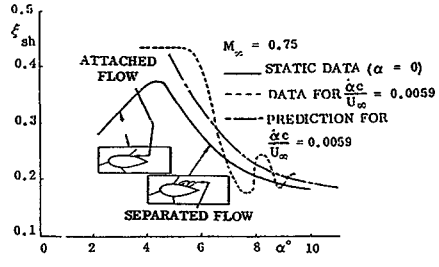

Fig. 17 Comparison between predicted[28] and measured[29] unsteady shock position.

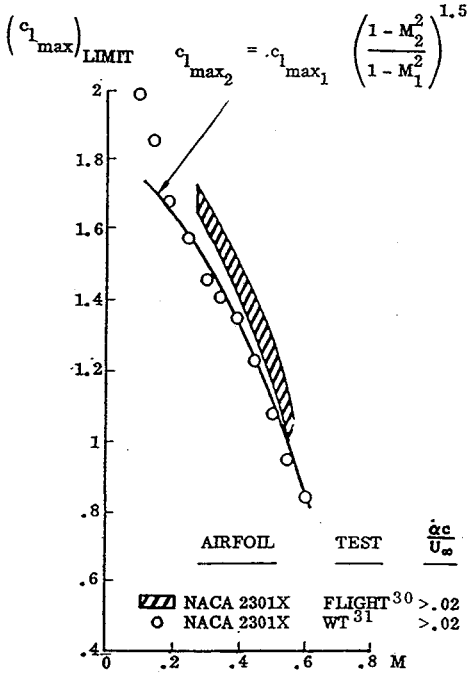

Fig. 18 Maximum lift as a function of Mach number for NACA 2301X airfoil.

subscribing fully to that explanation, it is necessary for CFD not only to produce results for $Re = 10^6$ similar to those in Fig. 15, but also to show that it can predict the large effect of nose radius demonstrated by the experimental results for a modified NACA 0012 airfoil[27] (Fig. 16). One explanation, based upon moving wall effects,[19] is that the oscillation observed on the basic NACA 0012 with its larger nose radius is caused by an oscillating separation point, similar to what has been observed for shock-induced flow separation[28,29] (Fig. 17). In the case of the sharper leading edge of the modified NACA 0012 airfoil, the initial overshoot of the static lift maximum is much more modest (Fig. 16), providing rather weak initial conditions for the oscillation of the flow separation point.[29] Compressibility has a similar effect. Increasing the subsonic Mach number will produce an apparent decrease of the nose radius,[10] $\rho_N \sim (1 - M_\infty^2)^{1.5}$, resulting in a rapid decrease of the dynamic lift maximum with increasing subsonic Mach number[30,31] (Fig. 18).

Conclusions

The general conclusion to be drawn from an analysis of experimental and numerical results for dynamic airfoil stall is that the present CFD technology cannot account for the moving wall effect on the unsteady aerodynamics of advanced aircraft. This is especially critical in the case of self-excited oscillations, such as wing rock, where the moving wall effect is dominant. Even in the case of so-called supermaneuvers, the moving wall effect is found to be very important, if not completely dominant, for angular rates representative of current and future high-performance aircraft.

References

[1]Chapman, D. R., "Dryden Lecture: Computational Aerodynamics Development and Outlook," *AIAA Journal*, Vol. 17, No. 12,

1979, pp. 1293–1313.

[2]Acharya, M., and Metwally, H. M., "Unsteady Pressure Field and Vorticity Production over a Pitching Airfoil," *AIAA Journal*, Vol. 30, No. 2, 1992, pp. 403–411.

[3]Visbal, M. R., "On Some Physical Aspects of Airfoil Dynamic Stall," American Society of Mechanical Engineers Symposium on Non-Steady Fluid Dynamics, Toronto, Canada, June 1990.

[4]Ericsson, L. E., and Reding, J. P., "Fluid Dynamics of Unsteady Separated Flow. Part II. Lifting Surfaces," *Progress in Aerospace Sciences*, Vol. 24, 1987, pp. 249–356.

[5]Ericsson, L. E., and Reding, J. P., "Fluid Mechanics of Dynamic Stall. Part I. Unsteady Flow Concepts," *Journal of Fluids and Structures*, Vol. 2, 1988, pp. 1–33.

[6]Daley, D. C., and Jumper, E. J., "Experimental Investigation of Dynamic Stall," *Journal of Aircraft*, Vol. 21, No. 10, 1984, pp. 831, 832.

[7]Ericsson, L. E., and Reding, J. P., "Dynamic Overshoot of Static Stall Angle," *Journal of Aircraft*, Vol. 22, No. 7, 1985, pp. 637, 638.

[8]Liiva, J., Davenport, F. J., Grey, L., and Walton, I. C., "Two-Dimensional Tests of Airfoils Oscillating Near Stall," U.S. Army Aviation Labs., TR 68-13, Fort Eustis, VA, April 1968.

[9]Scruggs, R. M., Nash, J. F., and Singleton, R. E., "Analysis of Flow-Reversal Delay for a Pitching Foil," AIAA Paper 74-183, Jan. 1974.

[10]Ericsson, L. E., and Reding, J. P., "Stall Flutter Analysis," *Journal of Aircraft*, Vol. 10, No. 1, 1973, pp. 5–13.

[11]Windsor, R. I., "Measurement of Aerodynamic Forces on an Oscillating Airfoil," U.S. Army Aviation Labs., TR 69-98, Fort Eustis, VA, March 1970.

[12]Ericsson, L. E., "Flow Reattachment on Wings in Pitch-Down Motion," International Council of the Aeronautical Sciences Paper 94-3.4.4, Sept. 1994.

[13]Ericsson, L. E., "Various Sources of Wing Rock," *Journal of Aircraft*, Vol. 27, No. 6, 1990, pp. 488–494.

[14]Fratello, D. J., Croom, M. A., Nguyen, L. T., and Domack, C. S., "Use of the Updated NASA Langley Radio-Controlled Drop-Model Technique for High-Alpha Studies of the X-29A Configuration," AIAA Paper 87-2559, Aug. 1987.

[15]Rainey, A. G., "Measurement of Aerodynamic Forces for Various Mean Angles of Attack on an Airfoil Oscillating in Bending with Emphasis on Damping in Stall," NACA TR 1305, 1957.

[16]Ericsson, L. E., "Effects of Transition on Wind Tunnel Simulation of Vehicle Dynamics," *Progress in Aerospace Sciences*, Vol. 27, 1990, pp. 121–144.

[17]Swanson, W. M., "The Magnus Effect: A Summary of Investigations to Date," *Journal of Basic Engineering*, Vol. 83, 1961, pp. 461–470.

[18]Carta, F. O., "A Comparison of the Pitching and Plunging Response of an Oscillating Airfoil," NASA CR-3172, 1979.

[19]Ericsson, L. E., "Moving Wall Effects in Unsteady Flow," *Journal of Aircraft*, Vol. 25, No. 11, 1988, pp. 977–990.

[20]Jacobs, E. N., and Sherman, A., "Airfoil Section Characteristics as Affected by the Reynolds Number," NACA TR 586, 1937.

[21]Ericsson, L. E., "Prediction of High-Alpha Vehicle Dynamics," International Council of Aeronautical Sciences Paper 90-3.5.1, Sept. 1990.

[22]Freymuth, P., "Vortices," *Handbook of Flow Visualization*, edited by W. Yang, Hemisphere, New York, 1989, Chap. IV-3.

[23]Herbst, W. B., "Supermaneuverability," *Proceedings of Workshop on Unsteady Separated Flow*, edited by Frances and Luttges, U.S. Air Force Academy, Colorado Springs, CO, pp. 1–9.

[24]Brandon, J. B., "Dynamic Stall Effects and Applications to High Performance Aircraft," Paper 2, AGARD-R-776, April 1991.

[25]Ericsson, L. E., and Reding, J. P., "Dynamic Stall at High Frequency and Large Amplitude," *Journal of Aircraft*, Vol. 17, No. 3, 1980, pp. 136–142.

[26]Ham, N. D., and Garelick, M. S., "Dynamic Stall Considerations in Helicopter Rotors," *American Helicopter Society Journal*, Vol. 13, April 1968, pp. 44–55.

[27]Carr, L. W., McAlister, K. W., and McCroskey, W. J., "Analysis of the Development of Dynamic Stall Based on Oscillating Airfoil Experiments," NASA TN D-8382, Jan. 1977.

[28]Ericsson, L. E., "Dynamic Effects of Shock-Induced Flow Separation," *Journal of Aircraft*, Vol. 12, No. 2, 1975, pp. 86–92.

[29]Lambourne, N. C., "Some Instabilities Arising from the Interaction Between Shock Waves and Boundary Layers," Aeronautical Research Council, London, C.P. 473, Feb. 1958.

[30]Harper, P. W., and Flanigan, R. E., "Investigation of the Variation of Maximum Lift for a Pitching Airplane Model and Comparison with Flight Results," NACA TN 1734, 1948.

[31]Harper, P. W., and Flanigan, R. E., "The Effect of Rate of Change of Angle of Attack on the Maximum Lift of a Small Model," NACA TN 2061, 1949.